Revista Brasileira de Física, Vol. 5, N.° 3, 1975

Neutron Reaction Characteristics in LiF Crystals Irradiation

C. A. PIMENTEL, L. **Q.** AMARAL, L. P. MOURA and P. **A.** FRIJGOLLI
Instituto de Fisica*, ***Universidade de*** São Paulo, São Paulo SP

Recebido em 15 de Abril de 1975

The mean effective cross sections of ^{6}Li for the (n, *u)* reaction were calculated for thermal, intermediate and fast neutrons; this reaction is dominant in damage production in LiF crystals. The actual neutron spectrum was determined from measurements of thermal, intermediate and fast neutron fluxes, in the core of the IEA-R1-2MW swimming pool reactor, in high fluence conditions, by the activation analysis of special detectors. Percent contributions for the $^{6}Li(n, a)\,^{3}H$ reaction were calculated taking into account neutrons in different energy intervals as well as percent contributions of different neutron interactions with LiF.

Foram calculadas seções de choque efetivas médias do ^{6}Li para a reação (n, a), com neutrons térmicos, intermediarios e rápidos; essa reação contribui predominantemente para a produção de defeitos em cristais de LiF. Para tanto, foi determinado o espectro real de neutrons a partir de medidas dos fluxos de neutrons térmicos, intermediarios e rápidos no caroço do reator tipo piscina IEA-R1-2MW, em situação de altas fluências, utilizando monitores especiais de ativação. Foram calculadas contribuições porcentuais para a reação $^{6}Li(n, \alpha)\,^{3}H$, considerando os diferentes intervalos de energia de neutrons, bem como contribuições porcentuais de diferentes interações de neutrons com LiF.

1. Introduction

The nature and number of defects induced in a crystal by irradiation depend on the particular interaction processes[1-4]. Lithium fluoride crystals were irradiated at different neutron fluxes and energy distributions in a swimming pool reactor by Pimentel[5] in order to study radiation damage. Therefore, it is necessary to consider all possible neutron and gamma rays interactions with Li and F. In these crystals, Li has its natural isotopic constitution (^{6}Li – 7.42%; ^{7}Li – 92.58%).

Usually, it is assumed that the $^{6}Li\,(n, \alpha)\,^{3}H$ reaction is dominant in the production of defects in LiF crystals by neutron irradiation[6], but

*Postal Address: Caixa Postal 20516, 01000 – São Paulo, SP

this assumption has not been rigorously discussed. Since the cross section $\sigma(E)$ is energy dependent, it is important to calculate an effective cross section σ_{eff}, for that reaction in the available neutron energy interval, weighted with the effective neutron flux distribution in energy @(E), according to:

$$\sigma_{eff} = \frac{\int \Phi(E)\,\sigma(E)\,dE}{\int \Phi(E)\,dE} \qquad \text{(b)} \qquad (1)$$

For calculating σ_{eff} and defining the irradiation conditions, necessary in quantitative radiation damage studies[2,5,7-9], a detailed knowledge of the functions $\Phi(E)$ and $\sigma(E)$ is needed in the energy interval of interest, that is, from 10^{-5} eV to 10 MeV, since the number of neutrons with energy outside this interval is negligible[10].

The cross section distributioii $\sigma(E)$ can be obtained from reported values for different neutron eneigy intervals. The cross section $\sigma(E)$ for $^{6}Li(n,a)^{3}H$ reaction presents a resonance at about 250 KeV and, above 1 KeV[11,12], departs from a $1/v$ distribution[13,14], v being the neutron velocity. In the 10 KeV < E < 10 MeV region, $\sigma(E)$ values are tabulated[15]; in the 1.4 KeV < E < 10 keV region, the values are given by Schwarz[16] and Mahaux''; for energies lower than 1.4 KeV, it can be assumed that $\sigma(E) \propto 1/v$ (Ref. 17), with $\sigma_{th} = 950$ b.

The neutron spectrum must refer to the actual neutron flux distribution $\Phi(E)$ of the specific irradiation conditions. In this paper, @(E) has been determined for the IEA-R1-2MW swimming pool research reactor.

The purpose of the present work is to determine $\Phi(E)$, σ_{eff} and to discuss the importance of the $^{6}Li(n,\alpha)^{3}H$ reaction in face of other interactions that may occur in LiF irradiation in a reactor. The importance of possible distortions in the $\Phi(E)$ spectrum is also discussed, to generalize the σ_{eff} results to other irradiation conditions. A general review of the determination of neutron fluences is also presented, because of its recognized importance in any experiment involving neutron in nuclear physics[18,19].

2. Neutron Fluence Measurements

Several methods, based on different neutron interaction processes, are used for neutron detection[20]. Those based on induced radioactivity

in special monitors are the most suitable for accurate measurements. In particular, for radiation damage studies, these activity rnonitors have some advantages: their small size allows the detection of neutron fluence practically at the same position of the sample; it is possible to integrate the flux over all the time of irradiation[5,7,9,21] and select the desired energy response.

In this paper we have employed activation detectors in order to measure thermal, intermediate and fast neutron fluxes in a high fluence condition: high flux (at reactor core) and long time irradiation (about 9 hours). Absolute and relative methods employed in this work, for activity measurements, are known and can be found in several papers[20] and in specific papers about neutron fluence measurements. Hence, details of the electronics used for counting will not be given here. The equipment used in the measurements has been previously described[22]. The outline of the activity method is given in the Appendix. Several special activity detectors were tested and the techniques will be discussed.

A) Thermal Neutron Fluence Measurements

In the present case, it is convenient to define thermal flux as the flux of neutrons with energies below 0.45 eV; this value corresponds to the cadmium threshold energy, E_{Cd}, for isotropic flux and the employed cadmium thickness.

Gold and cobalt are the usual detectors for thermal neutron fluences. For our purpose, Al-Co (Co: 0.475%) alloy was considered to be the most suitable thermal detector. This is a disk of 1 mm diameter, 0.5 mm thickness and 1 mg mass.

The reaction of interest in this alloy[23] is illustrated in Fig. 1.

The radionuclide of interest is the ^{60}Co, with a half-life of 5.26 years, a mean cross section $(o) = 38.7$ b and N about 10^{16} nuclides per detector. A disk with the above characteristics is considered the most favorable one for the activity measurement (3×10^3 counts per second) in the case of an irradiation time of about 9 hours and a flux of about 10^{13} n.cm^{-2}.s^{-1}. The activity was measured by absolute and relative methods; in the former case, it was employed the coincidence method[24] in a $4\pi\beta$-γ system. The relative activity was determined using the γ- radiation of a standard source of ^{60}Co, measured with a sodium

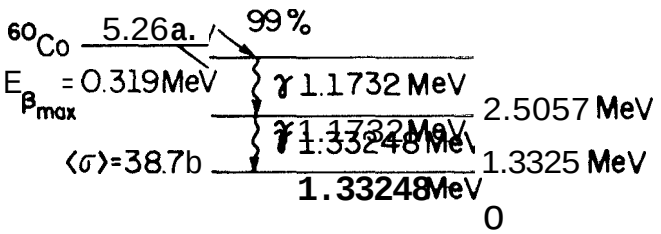

Fig. 1 - Reaction of interest in AI-Co monitor

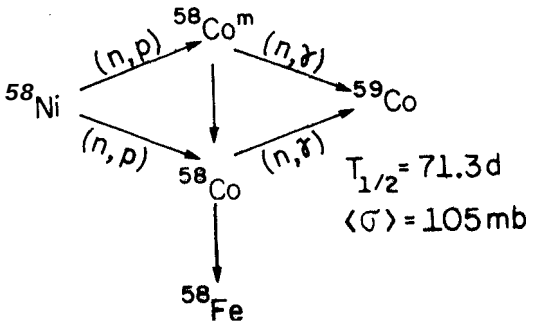

Fig. 2 - Reacíion of interest in Ni monitor

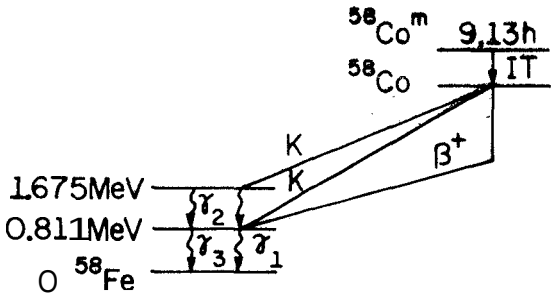

Fig. 3 - Disintegration scheme in Ni monitor

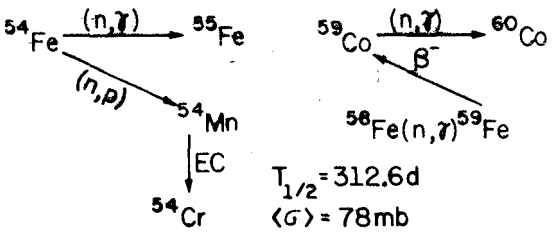

Fig. 4 - Reactions of interest in Fe monitor

iodine crystal with a defined geometry. This standard source was specially made with dimensions and activity as close as possible to that of the detector.

For both methods, within the experimental error, the measured value of the flux was practically the same. Due to the fact that the absolute method presents a higher accuracy in the flux value, this method was adopted in all the measurements.

The cadmium ratio R_{Cd} was determined by usual methods[9,20], from activity measurements of the irradiated detector covered and uncovered with cadmium, considering the usual corrections. The mean value obtained was $R_{Cd} = 10.8 \pm 0.4$.

The mean value obtained for the thermal neutron flux is:

$$\phi_{th} = (1.52 \pm 0.04) \times 10^{13}\ \mathrm{n \cdot cm^{-2} \cdot s^{-1}}.$$

Another possible way to measure high fluxes is to perform the measurement at the same position with low reactor power and to assume a linear variation of the fiux with reactor power. However, one measurement of the thermal neutron flux, employing a small disk of AI-Co (mass $\cong$ 16 mg), irradiated during an hour at nominal 2 kW reactor power, showed a discrepancy of about 100% when compared with the mean value of thermal flux. This discrepancy must be due to two main uncertainties: the short time of irradiation and, to a larger extent, the fluctuations of the reactor power value. This result has shown that this procedure is in fact not reliable and was discarted.

B) Intermediate Neutron Fluence Measurements

The technique for measuring neutron fluence in this energy region is not as well established as that in thermal and fast neutron regions. Due to cross section variations in this resonance region for most elements, sandwich foil techniques[9,20] are commonly employed.

The flux ϕ_i is given by:

$$\phi_i = \int_{E_{Cd}}^{\infty} \Phi_i(E)dE = k \int_{E_{Cd}}^{\infty} \frac{dE}{E} = kI\ \mathrm{n \cdot cm^{-2} \cdot s^{-1}},$$

where I can be determined numerically and k is the scale factor, experimentally obtained by[9,20]:

$$k = \frac{\frac{(A_0)_n}{N} \cdot \frac{(A_0)_{Cd}}{(N)_{Cd}}}{[1 - \exp(-\lambda t_i)]\,[(R)_{Cd} - 1] \int_{0{\cdot}45}^{\infty} \frac{\sigma(E)}{E}\, dE},$$

where $(A_0)_n$ and $(N)_{Cd}$ are the saturation activity and the number of target nuclei in the sample with the cadmium shield, respectively. The deterrnination of k involves the determination of $(R)_{Cd}$ for the monitor used and the knowledge of the resonance activation integral.

Two disks of Al-Co(0.475 %) alloy ($\sim$ 1 mg mass) were irradiated together, one of them being covered with cadmium. Special care was taken in order to avoid shadow effects. The corrections for the thickness of the cadrnium shield were considered and the $(R)_{Cd}$ value used was the same as the one given for thermal neutron, since the same monitor was employed. The reaction of interest in this alloy has been previously described in this work.

The resonance integral for ^{60}Co is given by[9]:

$$\int_{0{\cdot}45}^{\infty} \frac{\sigma(E)}{E}\, dE = (50 \pm 12)\ \text{b},$$

resulting a value of $k = 1.23 \times 10^{12}$.

The I integral value was calculated numerically, taking 1 keV intervals. Since for E > 1 MeV the contribution of the function $\Phi_i(E)$ is negligible compared to function $\Phi_f(E)$ of the fission spectrum[5], $E_i = 1$ MeV was taken as the upper limit of the integral I. The resulting value for this integral is 14.865 n . cm^{-2} . s^{-1}.

The value obtained for the intermediate flux is:

$$\phi_i = (1.9 \pm 0.1) \times 10^{13}\ \text{n} \cdot \text{cm}^{-2} \cdot \text{s}^{-1}.$$

C) Fast Neutron Fluence Measurements

This deterrnination can be done employing a threshold activation detector, *i.e.*, using the activity due to reactions that occur only above

a given neutron energy value. This value is a characteristic of a particular reaction in the material of the detector.

The conventions used to report fast neutron fluence are more ambiguous than those used for thermal and intermediate neutron, since fast neutron thresholds differ from one monitor material to another. So, it is important to pay attention to the differential cross section curves of the threshold reaction in order to know the interval of neutron distribution which is detected and, consequently, how accurate the fluence determination is.

In radiation damage it is of particular importance to have monitors sensitive to neutrons with energies around 1 MeV, due to the convention commonly used in this research field[9]; this leads to monitors with threshold energy about 1 MeV.

Among the many threshold reactions observed by irradiation, only a few are suitable for fluence measurements, and the $^{58}Ni(n, p)^{58}Co$ and $^{54}Fe(n, p)^{54}Mn$ reactions are widely used[23], both of them showing threshold energies around 1 MeV.

Two detectors, both available from the International Atomic Energy Agency, were employed with success, and the determination of the activity of the irradiated monitors was done by comparison with calibrated standard sources also available from the IAEA. The overall uncertainty of the standards is about $\pm 1\%$ (Ref. 23).

The measurements were done in a NaI spectrometer, taking precautions in order to maintain the geometry of the system using, for instance, empty aluminium containers of the same type as the ones where the standard source is sealed.

The material constants and disintegration data for Ni and Fe monitors, were obtained from Kohler[23].

a) Ni Monitor

The reaction of interest is shown in Fig. 2, and the disintegration scheme in Fig. 3.

The Ni (pure) is available in the form of disks (10 mm diameter, 0.05 mm thickness) and wires (10 mm long, 0.125 mm diameter). In the expe-

rimental conditions, the Ni was considered a good monitor due to its half-life, the reaction cross section and the easiness in the relative determination of activity. For the disk, N $\geq 10^{20}$ nuclides, C = 2 x 10^3 cps and for the wire, N $\geq 10^{19}$ nuclides, C = 10^2 cps. These counts refer to the measurement setting of the window of the spectrometer at the photopeak of 1.1 MeV and 1.3 MeV gamma. The C value (cps) obtained for the disk is more adequate than that obtained for the wire.

After a cooling time of about two days, the main activity remaining in the nickel monitor is due to ^{58}Co (Ref. 23).

The correction due to the burn-up of ^{58}Co was estimated and it was found to be negligible for the particular thermal flux of $\sim 10^{13}$ n.cm^{-2}.s^{-1} and the total time of irradiation of $\sim$ 9 hours.

b) Fe Monitor

The reactions of interest are given in Fig. 4 and the disintegration scheme[23] in Fig. 5.

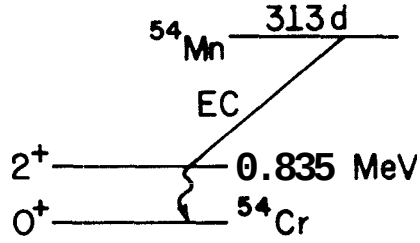

Fig. 5 - Desintegration scheme in Fe monitor

The Fe(pure) is available in the form of a disk, similar to that of Ni. The Fe monitor would be as good as the one of Ni if its measurement techniques were less complex. (N $\cong 10^{19}$ nuclides and C = 2 x 10^2 cps).

In this monitor, it is produced, in addition to ^{54}Mn, an approximately equal quantity of ^{59}Fe and, depending on the thermal flux level and on the irradiation time, also ^{60}Co. In general, a straight measurement is not possible due to the fact that in the NaI(Tl) gamma ray spectrometer the 835 KeV total absorption peak of the ^{54}Mn is superimposed on the Compton continuum of the 1.10 and 1.29 MeV gamma rays of ^{59}Fe and of the 1.17 and 1.33 MeV of ^{60}Co.

The routine measurement can be easily performed, using multichannel analyser data to obtain the activity of ^{54}Mn (Ref. 23).

Using a standard source of ^{59}Fe, it is possible, by adequate discrimination, to evaluate the ratio between the counts due to the Compton and the photoelectric effects of the gammas of ^{59}Fe. This ratio allows the elimination of the Compton counting of ^{59}Fe in the monitor; the ^{54}Mn activity is then obtained comparing its counting rate with that of a ^{54}Mn standard source. The mean value obtained in this way for the fast neutron flux is:

$$\phi_f = (6.5 \pm 0.2) \times 10^{12}\ \mathrm{n\,.\,cm^{-2}\,.\,s^{-1}}.$$

D) Summary of Fluence Results

Table I shows the mean value of thermal, intermediate and fast neutron fluxes, at the EIFS – 35 **A** (shelf 5) position[5], with the irradiation elements arranged in the pattern 88, and the Reactor IEA-R1 operating at 2 MW power. The monitors were subjected to an irradiation of about 9 hours.

For each flux and fluence value, it was calculated an error, from the propagation of the precision indices of all the physical quantities involved. The errors in the thermal, intermediate and fast flux are of about 5% or less. The errors shown in Table I refer to a weighted standard error of the mean value[25]. These errors are not only due to imprecision in the measurement but they also account for the reactor fluctuation over several months.

3. Neutron Flux Distribution in Energy

The neutron flux distribution in energy or neutron flux density $\Phi(E)$ is proportional to a normalized $D(E)$ distribution:

$$\Phi(E) = k\,.\,D(E)\ \ \mathrm{n\,.\,cm^{-2}\,.\,s^{-1}\,.\,eV^{-1}},$$

where k is a constant of proportionality, related to a particular condition of neutron flux density.

The number of neutrons in any generic energy interval is given by:

$$\phi = \int_{E_i}^{E_f} \Phi(E)\,.\,dE = k\,.\int_{E_i}^{E_f} D(E)\,.\,dE = \mathrm{k\ n\,.\,cm^{-2}\,.\,s^{-1}},$$

THERMAL $0.45\,eV < E_n$		INTERMEDIATE $0.45\,eV < E_n < 1\,MeV$		FAST $1\,MeV < E_n < 10\,MeV$	
Flux $n.cm^{-2}.s^{-1}$	Fluence $n.cm^{-2}$	Flux $n.cm^{-2}.s^{-1}$	Fluence $n.cm^{-2}$	Flux $n.cm^{-2}.s^{-1}$	Fluence $n.cm^{-2}$
$(1.52 \pm 0.04) \times 10^{13}$	$(4.9 \pm 0.2) \times 10^{17}$	$(1.9 \pm 0.1) \times 10^{13}$	$(6.1 \pm 0.3) \times 10^{17}$	$(6.5 \pm 0.2) \times 10^{12}$	$(2.11 \pm 0.07) \times 10^{17}$

Table I - Thermal, intermediate and fast neutron fluxes and fluences at IEA-R1, EIFS-35-A (shelf 5), 2MW power reactor. Fluences refer to 9 hours of irradiation.

where ϕ is the actual experimentally obtained neutron flux and I can be numerically determined by integration of the $D(E)$ function.

From these two integrals, the scale factor k can be obtained, since $k = \phi/I$.

The total neutron spectrum can be subdivided into three components:

$10^{-5}\,\text{eV} < \text{E} < 0.45\,\text{eV}$ – thermal neutron spectrum, Φ_{th}
$0.45\,\text{eV} < \text{E} < 1\,\text{MeV}$ – intermediate neutron spectrum, Φ_i
$1\,\text{MeV} < \text{E} < 10\,\text{MeV}$ – fast neutron spectrum, Φ_f.

Neutrons in thermal equilibrium with the moderator obey approximately a Maxwellian distribution of neutron density[g]

$$D_{\text{th}}(E) = \frac{E}{E_0^2}\exp\left(-\frac{E}{E_0}\right)\text{n}\,.\,\text{cm}^{-2}\,.\,\text{s}^{-1}\,.\,\text{eV}^{-1}.$$

Since the interest is in a mean effective cross section, it may be assumed that thermal neutrons obey a Maxwellian distribution, peaked at $E_0 = 0.0265\,\text{eV}$ corresponding to $\text{T} = 308 \pm 5\,\text{K}$, the actual moderator temperature.

At the reactor core, the density of fast neutron flux is proportional to the U_{235} fission spectrum[g]:

$$D_f(E) = \left(\frac{2}{2\pi}\right)^{1/2} e^{-E}\sinh(2E)^{1/2}\ \text{n}\,.\,\text{cm}^{-2}\,.\,\text{s}^{-1}\,.\,\text{MeV}^{-1}.$$

The intermediate neutron density distribution is inversely proportional to E (Ref. 9):

$$D_i(E) = 1/E\ \text{n}\,.\,\text{cm}^{-2}\,.\,\text{s}^{-1}\,.\,\text{eV}^{-1}.$$

The I integral values were numerically calculated, considering 0.0001 eV intervals for thermal neutrons and 0.01 MeV intervals for fast neutrons and are shown in Table II. Thermal and fast neutron fluxes, experimentally determined as explained before, are also shown in Table II. These values determine k; the scale factors for thermal and fast neutrons are shown in Table II.

Since the effective scale factors for fast and thermal neutron spectra are already determined, the neutron intermediate spectrum scale should

Region	Flux ϕ $n.cm^{-2}.s^{-1}$	Integral I $n.cm^{-2}.s^{-1}$	Scale factor k
Thermal	1.52×10^{13}	7.02×10^{-4}	2.16×10^{16}
Intermediate	–	–	1.23×10^{12}
Fast	6.5×10^{12}	6.69×10^{-5}	9.71×10^{16}

Table II. Values of neutron flux ϕ, integral I and scale factor k.

be taken from them. Nevertheless, around 0.45 eV and 1 MeV, the thermal and fission spectra are disturbed by the contribution of the $1/E$ component, making difficult the definition of the position of the $1/E$ function. Therefore, an experimental determination of the intermediate scale factor k_i was carried out, involving the determination of thermal neutron density, cadmium ratio $(R)_{Cd}$ and the knowledge of the resonance activation integral of the special activity detector employed. The obtained value is also given in Table II.

From $D(E)$ functions and k scale factors, the effective neutron flux distribution $\phi(E)$ was obtained in the whole energy interval and the result is shown in Figure 6.

In the disturbed spectrum region, the values adopted for @(E)were:

near 0.45 eV: $\Phi(E) = \Phi_{th}(E) + \Phi_i(E)$;
near 1 MeV: @(E)= $\Phi_i(E) + \Phi_f(E)$.

4. Mean Effective Cross Section for $^6Li(n, \alpha)^3H$ Reaction

The @(E)neutron spectrum and the cross section $\sigma(E)$ for $^6Li(n, \alpha)^3H$ reaction are shown in Figure 6, in a double logarithmic scale.

The mean values, $\sigma_{eff}(E)$, were numerically determined according to expression (1), for thermal, intermediate and fast neutron groups. The σ_{eff} values and the percent contribution of neutrons, in different energy intervals for the $^6Li\,(n, \alpha)\,^3H$ reaction are given in Table III. The mean effective cross section related to intermediate plus fast neutrons was also calculated, assuming the limits of integration as E = 0.45 eV and E = 1 MeV, and by a simple sum of both mean effective cross sections;

References

1. J. H. Varley, Peaceful use of Atomic Energy, 7, 642 (1955).
2. D. S. Billington, Peaceful use of Atomic Energy, 7, 421 (1955).
3. B. Gruber, *Theory of Crystal Defects,* Academic Press, N. Y. (1966).
4. M. W. Thompson, *Defects and Radiation Damage in Metals,* Cambridge at the University Press (1969).
5. C. A. Pimentel, Thesis, Universidade de São Paulo (1973).
6. D. T. Keating, Phys. Rev. 97, 832 (1955).
7. D. S. Billington and J. H. Crawford Jr., *Radiation Damage in Solids,* Princeton, 77 (1961).
8. A. Seeger, *Theory of Crystal Defects* in *Proceeding of the Summer School held in Hrazany in September* – Academic Press, N. Y., 343 (1964).
9. *Neutron Fluence Measurements* – Technical Reports n.º 107; IAEA, Vienna (1970).
10. W. J. Price, *Nuclear Radiation Detection,* Mc Graw-Hill Book Co., Inc., 38 (1958).
11. C. Mahaux and G. Robaye, Nucl. Phys. 74, 161 (1965).
12. R. B. Murray and H. W. Schmitt, Phys. Rev. 115, 1707 (1959).
13. S. J. Bame and R. L. Cubitt, Phys. Rev. 114, 1580 (1959).
14. A. A. Bergman and F. L. Shopiro, Sov. Phys. Jetp 13, 895 (1961).
15. J. R. Stehn, M. D. Goldberg, B. A. Magurno and R. Wiener – Chasman, BNL-325, Suppl. n.º 2 (1964).
16. S. Schwarz, L. G. Stromberg and A. Bergstrom, Nucl. Phys. **63,** 593 (1965).
17. D. J. Hughes, *Pile Neutron Research,* Addison Wesley Publishing Co., Inc. 6 (1953).
18. H. Goldstein, *Fundamental Aspects of Reactor Shielding,* Addison Wesley, 133 (1959).
19. R. W. Durban, *Proceedings of the International Conference Modern Trends in Activation Analysis,* (1961).
20. W. J. Price, *Nuclear Radiation Detection,* McGraw-Hill Book Co., 311 (1958).
21. *Radiation Damage in Reactor Materials,* Vol. 1 and II, IAEA (1969)
22. L. P. Moura and D. C. C. Reis, Informe IEA n.º 152 (1968).
23. W. Kohler, IAEA/RL/1D, (1971).
24. L. P. Moura, Thesis, Instituto de Física da UNICAMP (1969).
25. P. J. Campion, J. E. Burns and A. Williams, *A code of practice for the detailed statement of accuracy,* National Physical Laboratory, London (1973).
26. S. Glasstone and M. C. Edlund, *The Elements of Nuclear Reactor Theory,* D. Van Nostrand, 339 (1952).
27. T. Lauritsen and F. Ajznberg-Selove, Nucl. Phys. 78, 1 (1966).
28. D. J. Hughes and J. A. Harvey, BNL-325 (1955).
29. D. J. Hughes, B. A. Magurno and M. K. Brussel, BNL-325, Suppl. n.º 1 (1960).
30. M. E. Battat, D. J. Dudziak and R. J. LaBauve, LA 3695 (1967).
31. G. M. Frye Jr., Phys. Rev. 93, 1086 (1954).
32. G. F. Dienes and G. H. Vineyard, *Radiation Effects in Solids,* N. York, Interscience (1957).
33. E. Troubetzkoy and H. Goldstein, ORNL-2904 (1961).
34. M. T. F. Cesar, M. S. Dissertation, Universidade de São Paulo (1970).
35. R. W. Christy, N. M. Johnson and R. R. Wilbary, J. Appl. Phys. 38 2099 (1967).
36. F. Gabbard, R. H. Davis and T. W. Bonner, Phys. Rev. 114, 201 (1959).